Reactivity of ultra-thin ZnO films supported by Ag(111) and Cu(111): A comparison to ZnO/Pt(111).

Q. Pan,[1,2] B.H. Liu,[1] M.E. McBriarty,[1,3] Y. Martynova,[1] I.M.N. Groot,[1] S. Wang,[2] M.J. Bedzyk,[3] S. Shaikhutdinov,[1*] H.-J. Freund[1]

[1]*Dept. of Chemical Physics, Fritz Haber Institute, Faradayweg 4-6, 14195 Berlin, Germany*

[2]*Dalian National Laboratory for Clean Energy, Dalian Institute of Chemical Physics, Chinese Academy of Science, Dalian 116023, Liaoning, China*

[3]*Dept. of Materials Science and Engineering, Northwestern University, 2220 Campus Drive, Evanston, IL, 60208-3108 USA*

Abstract. We studied structure and reactivity of ZnO(0001) ultrathin films grown on Ag(111) and Cu(111) single crystal surfaces. Structural characterization was carried out by scanning tunneling microscopy, Auger electron spectroscopy, low-energy electron diffraction, and temperature programmed desorption. The CO oxidation behavior of the films was studied at low temperature (450 K) at near atmospheric pressures using gas chromatography. For ZnO/Cu(111), it is shown that under reaction conditions ZnO readily migrates into the Cu crystal bulk, and the reactivity is governed by a CuO_x oxide film formed in the reaction ambient. In contrast, the planar structure of ZnO films on Ag(111) is maintained, similarly to the previously studied ZnO films on Pt(111). At sub-monolayer coverages, the "inverse" model catalysts are represented by two-monolayer-thick ZnO(0001) islands on Pt(111) and Ag(111) supports. While the CO oxidation rate is considerably increased on ZnO/Pt(111), which is attributed to active sites at the metal/oxide boundary, sub-monolayer ZnO films on Ag(111) did not show such an effect, and the reactivity was inhibited with increasing film coverage. The results are explained by much stronger adsorption of CO on Pt(111) as compared with Ag(111) in proximity to O species at the oxide/metal boundary. In addition, the water-gas shift and reverse water-gas shift reactions were examined on ZnO/Ag(111), which revealed no promotional effect of ZnO on the reactivity of Ag under the conditions studied. The latter finding suggests that wetting phenomena of ZnO on metals does not play a crucial role in the catalytic performance of ZnO-based real catalysts in those reactions.

Keywords: Thin oxide films; Zinc oxide; Inverse catalysts; CO oxidation.

1. Introduction

It has recently been demonstrated that ultra-thin films of transition metal oxides, either formed on a metal surface in an oxygen ambient or epitaxially grown on a different metal support, may exhibit interesting catalytic properties [1-5]. In particular, Ru-oxide films on Ru(0001)[6-8] and oxide films on Pt(111)[9-11] show a higher CO oxidation rate at near-atmospheric pressures and low temperatures at which pure metals are essentially inactive. The promotional effect of oxide overlayers on the reactivity observed on model planar systems allows one to rationalize the enhanced reactivity observed on highly dispersed metal particles, encapsulated by the supporting oxide due to the a so-called strong metal-support interaction, as has been demonstrated for iron oxide-supported Pt catalysts [12].

To better understand the role of a thin oxide film in such "monolayer" catalysts, one certainly needs comparative studies of different systems where the oxide composition, film thickness, and metal support are varied in a systematic manner. We recently studied the structure and reactivity of zinc oxide and manganese oxide thin films grown on Pt(111)[9, 13]. By comparison with other films, we concluded that oxygen binding energy in the films plays the decisive role for the CO oxidation reaction in an excess of oxygen [11]. The more weakly bound the oxygen species, the higher the reaction rate. More specifically, for Pt(111)-supported well-ordered films, the activity follows the trend FeO > MnO > ZnO. Although closed ZnO films on Pt(111) showed the lowest activity among the films studied, the films which only partially covered the Pt support showed a higher reaction rate than the closed films by a factor of 5 – 7. Such an enhancement is rationalized in terms of the reactions occurring at the oxide/metal boundary which are commonly studied using so called "inverse" model catalysts [14, 15].

To see whether a similar scenario can be applied to other metal supports, we address here the reactivity of ZnO films grown on Ag(111) and Cu(111) for comparison with ZnO/Pt(111). The work was also motivated by the fact that Cu/ZnO and Ag/ZnO catalysts show superior activity in methanol synthesis, and recent evidence suggests that the ZnO/Cu interface is responsible for this activity [16]. Note that encapsulation-derived structures have often been considered as active phases in methanol synthesis (see, for example, refs. [17-19]). Therefore,

planar ZnO films supported on Cu and Ag could be well suited for understanding the role of ZnO in those catalysts.

The preparation of ZnO films on low index Ag surfaces (Ag(100), Ag(110), and Ag(111)) was first studied by Kourouklis and Nix [20]. The films were grown by oxidation of ultrathin zinc films deposited at room temperature. The oxides formed at 300 K showed no long-range order, but upon heating to 500 K surface structures analogous to the polar surfaces of bulk ZnO(0001) were observed. Well-ordered ZnO films on Ag(111), prepared by pulsed laser deposition and vacuum annealing at 680 K, were used by Tusche et al.[21] to provide evidence for a theoretically predicted [22] depolarized ZnO(0001) structure, i.e. where Zn and O atoms are arranged in planar sheets as in the hexagonal boron-nitride structure.

The preparation of ZnO films on Cu singe crystal surfaces has been reported in many publications (see, for example, refs. [23-27]) in an attempt to fabricate an adequate model system for methanol synthesis catalysts. In most cases, the films were prepared by post-oxidation of a Zn overlayer deposited onto a clean or O-precovered Cu surface. However, the preparation of well-ordered ZnO films was not achieved.

In this work, well-defined ZnO(0001) films were grown on Ag(111) and Cu(111). These films were studied in the CO oxidation reaction at near-atmospheric pressures as a function of ZnO coverage in order to compare with the ZnO/Pt(111) system previously studied in our group [13]. The structural characterization of the model catalysts was performed by scanning tunneling microscopy (STM), Auger electron spectroscopy (AES), low-energy electron diffraction (LEED) and temperature programmed desorption (TPD), whereas the reactivity was monitored by gas chromatography (GC).

2. Experimental

The experiments were performed in two ultrahigh vacuum (UHV) chambers (base pressure below 2×10^{-10} mbar), both equipped with LEED, AES (both from Specs), and quadrupole mass-spectrometers (QMS, from Hiden) for TPD measurements. One chamber houses a high-pressure reaction cell for reactivity studies at atmospheric pressures using a

conventional GC (from Agilent) for gas composition analysis. The single crystal (double-side polished Ag(111), Pt(111), or Cu(111)) was spot-welded to thin Ta wires for resistive heating. The second chamber is additionally equipped with a STM (from Omicron) and has an Au-plated cell, separated from the main chamber by the gate-valve, for high-pressure treatments at the same reaction conditions as used for reactivity measurements. The sample crystal is clamped to an Omicron sample holder. In both setups, the sample temperature was measured by a Type K thermocouple spot-welded to the edge of the crystal.

Clean crystal surfaces were obtained by cycles of Ar^+ sputtering and annealing in UHV and 10^{-7} mbar O_2. The cleanliness was checked by AES. Zinc was vapor deposited by heating a Zn rod (1 mm in diameter, 99.99%, from Goodfellow) to ~ 520 K using a tungsten wire wrapped around the rod. The Zn source was shielded by a stainless cylinder having a ~ 5 mm orifice and placed ca. 2 cm away from the crystal. The deposition flux was controlled via a Type K thermocouple spot-welded to the edge of the Zn rod.

On Pt(111), the zinc oxide films were prepared by Zn deposition in 10^{-7} mbar O_2 followed by oxidation at 600 K in 10^{-6} - 10^{-5} mbar O_2 for 20 min. For Ag(111) or Cu(111) supports, the zinc oxide films were prepared by Zn deposition in 10^{-5} mbar O_2 followed by UHV annealing at 600 K or 500 K, respectively, for 10 min.

The reaction mixture for CO oxidation consisted of 10 mbar CO and 50 mbar O_2. For the water-gas shift reaction, the mixture contained 3 mbar CO and 3 mbar H_2O. For the reverse water-gas shift reaction, the reactants included 50 mbar CO_2 and 50 mbar H_2. The reaction gas mixture, balanced by He to 1 bar, was dosed at room temperature and slowly circulated for 20 min. Then the sample was heated to 450 K (for CO oxidation) or 500 K (for the water-gas shift and reverse water-gas shift reactions) with a rate of 1 Ks^{-1}, and reaction was monitored by GC.

3. Results and discussion

First we briefly recall the key results observed for the previously studied ZnO/Pt(111) system [13]. The “as prepared“ films showed a monolayer ZnO(0001) structure (i.e. consisting of single layers of Zn and O), forming a Pt(111)-(6x6) Moiré pattern, although the ZnO surface

termination could not be determined by the experimental tools available (LEED, AES, STM). Under CO oxidation conditions in an O_2-rich ambient (10 mbar CO, 50 mbar O_2, He balance to 1 bar, 450 K), monolayer islands and an entire monolayer film transformed into two-monolayers thick (i.e. bilayer) islands, which dominate the surface of the active catalysts. The CO_2 production rate over the films reached a maximum at a surface coverage of about 70 % and was attenuated as the nominal film thickness further increased. The ZnO(0001) film grew in a layer-by-layer mode. Note that the surface coverage was determined by CO titration of Pt (for sub-monolayer coverage) in combination with AES (for the closed films).

3.1. Structure and reactivity of ZnO(0001) on Ag(111)

Now we address the reactivity of thin ZnO films on Ag(111) performed under the same conditions and in the same setup as used for ZnO/Pt(111). Since Zn readily forms surface alloys with Ag, the films were prepared by Zn deposition in an oxygen ambient to prevent intermixing. Then the films were annealed in UHV at 600 K (see Experimental). Figure 1 displays an STM image and a LEED pattern of the “as prepared” film partially covering the Ag(111) surface. The diffraction spots of ZnO are aligned with those of Ag(111) and correspond to the ZnO(0001) surface with a lattice constant of 0.325 nm. The ZnO overlayer is clearly visible in STM through the characteristic Moiré corrugation modulation caused by the ZnO(0001)-(7x7)/Ag(111)-(8x8) coincidence structure, which has a ~ 2.3 nm periodicity. Although a few domains often coexist on one terrace, the resulting ZnO film surface is atomically smooth. However, the precise assignment of whether ZnO forms a mono- or bi-layer structure is uncertain from analysis of step heights. Therefore, we used AES results, first calibrated by STM on the ZnO/Pt(111) samples, where mono- and bi-layer islands could be clearly discriminated [13]. The results suggest that the ZnO islands on Ag(111) primarily grow as bilayers, albeit the interfacial layer can be embedded into the Ag terrace (more details will be presented in ref. [28]). (It is noteworthy that a similar picture has been invoked for NiO(100) films on Ag(100)[29]).

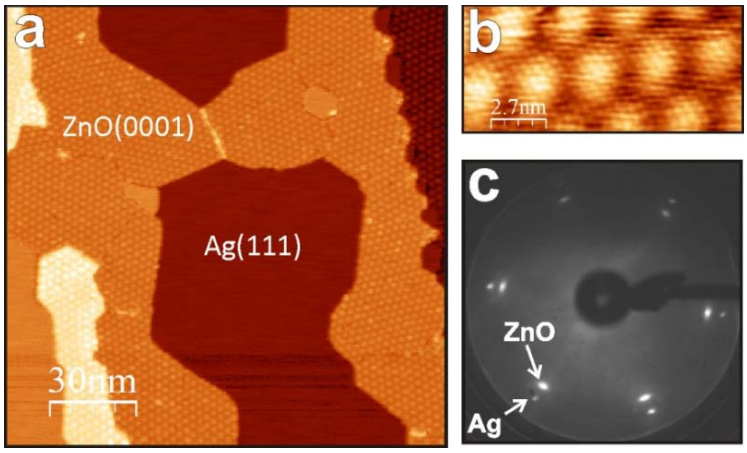

Figure 1. (a, b) STM images of a ZnO(0001) film on Ag(111). Tunneling bias 1.5 V, current 0.6 nA. (c) Respective LEED pattern (at 60 eV).

The similarly prepared ZnO/Ag(111) samples were examined in the CO oxidation reaction in the other UHV setup. In the absence of STM, determination of the film coverage by titration experiments is very uncertain. The Ag(111) surface is essentially inert to many probe molecules, and their physisorption occurs at low temperatures where it overlaps with that of ZnO. Therefore, we employed AES and LEED to estimate oxide coverage in the samples used for reactivity studies.

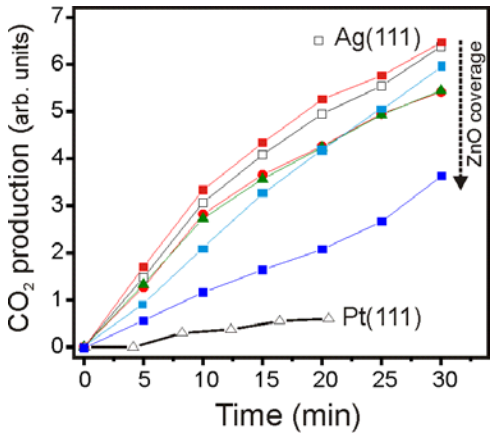

Figure 2. Integrated CO_2 production over ZnO/Ag(111) model catalysts. The film coverage ranges from 0.1 to about 1 ML, as indicated. The results for pristine Ag(111) and Pt(111) are shown for comparison. (Reaction conditions: 10 mbar CO, 50 mbar O_2 (He balance to 1 bar); 450 K).

Figure 2 displays kinetics of CO_2 production over clean and ZnO-covered Ag(111) crystal surfaces at 450 K. Interestingly, the pristine Ag(111) crystal shows a higher activity than Pt(111) under the same conditions. This finding could likely be explained by a much stronger CO adsorption on Pt than on Ag, which blocks the O_2 dissociation. The low-coverage ZnO films showed essentially no or a slightly inhibiting effect on reactivity. Only at high coverages is the activity substantially decreased. Notably, the results revealed considerable data scattering at the low ZnO coverages, such that it was difficult to precisely establish the coverage dependence. It therefore appears that the reactivity depends on the precise morphology of ZnO/Ag(111) surfaces. Post-characterization of the spent catalysts by LEED and AES in comparison with the "as prepared" samples revealed no considerable changes. The LEED patterns of the ZnO/Ag(111) and clean Ag(111) model catalysts after reaction still showed diffraction spots of ZnO(0001) and Ag(111); however, those of Ag(111) were more strongly attenuated than of ZnO when compared with the LEED pattern before the reaction (see Fig. S1 in Supplementary Information). Also, Auger spectra showed basically the same film stoichiometry, although the reacted surfaces became lightly contaminated with carbon. Finally, STM studies of the films, treated at elevated pressures and temperatures to mimic the reaction conditions, did not reveal any considerable dewetting of the films, in agreement with the LEED and AES results. Note, however, that STM did show some roughening of the ZnO surface, as was the case for ZnO/Pt(111) (Fig. S2a).

Taken together, these results suggest that the reactivity of the clean Ag(111) surface seems to be associated with specific (defect) sites rather than regular terrace sites, which are well known to exhibit very low sticking coefficients for both CO and O_2 molecules [30, 31]. Indeed, reactivity measurements carried out over a highly roughened Ag(111) crystal revealed a considerably higher (by a factor of two) reaction rate than the perfect crystal studied here. Depending on the ZnO coverage, these sites could be poisoned by ZnO. All in all, the results clearly show no promotional effects of ZnO on CO oxidation over Ag(111) under our conditions.

3.2. Structure and reactivity of ZnO(0001) on Cu(111)

The preparation of crystalline ZnO films on Cu(111) was very similar to that used for Ag(111) except that the annealing temperature was lowered to 500 K to obtain well-ordered films (the details will be presented in ref. [32]). In general, the ZnO films grown on Cu(111) showed smaller domains than those observed on Ag(111), probably due to a larger lattice mismatch between ZnO(0001) and Cu(111) as compared with ZnO/Ag(111) (27.5 % and 12.5 %, respectively). STM images indicated the formation of ZnO(0001) mono- and bi-layer structures. As in the case for the Ag(111) support, the films on Cu(111) left exposed substrate metal patches even at ~ 2 ML coverage (Fig. 3).

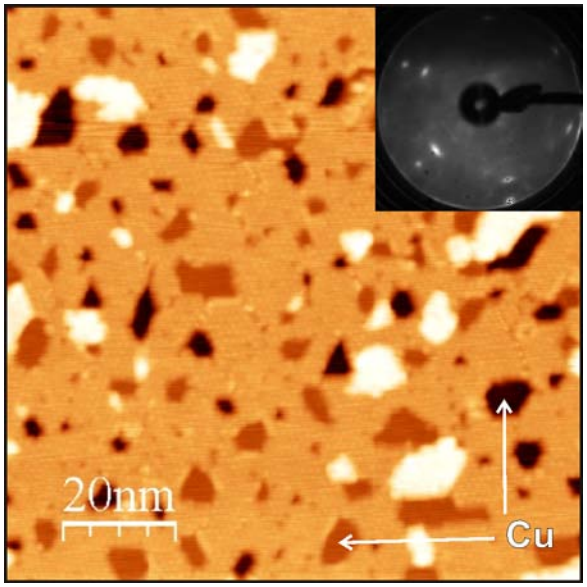

Figure 3. STM image of a 2 ML ZnO(0001) film on Cu(111). The film left exposed substrate metal patches (as indicated by arrows). Tunneling conditions: bias 1.2 V, current 0.6 nA. The inset shows a corresponding LEED pattern at 60 eV.

The reactivity data for the clean Cu(111) and ZnO/Cu(111) surfaces are summarized in Fig. 4. First, we note that the reaction over pristine Cu(111) exhibits a rate acceleration in the first 20 minutes which is apparently missing on Ag(111) (see Fig. 2). This indicates some considerable surface restructuring. Indeed, LEED inspection of the sample after the catalytic

test did not show any diffraction spots, thus suggesting severe surface disordering. In contrast to Ag(111), the Cu(111) surface is readily oxidized at elevated oxygen pressures and temperatures as clearly seen in Figure 5, which shows AES spectra of the Ag(111) and Cu(111) surfaces before and after the reaction. Therefore, it seems plausible that the observed induction period on Cu(111) is associated with the formation of a Cu-oxide overlayer. For comparison, we have examined a well-ordered Cu-oxide ultrathin film, which is referred to in the literature as the "44"-Cu_2O/Cu(111) structure [33]. Figure 4 shows that only the initial rate slightly increased, thus indicating that the Cu precursor state is not critical for the observed steady state reactivity over Cu(111). Again, the spent catalysts showed no long-range order in LEED and revealed a substantial increase in the oxygen present on the surface as compared to the "44"-Cu_2O surface. Finally, STM inspection of the reacted films revealed a very rough surface morphology with up to 10 nm corrugation (Fig. S2b). Therefore, the reactivity of Cu(111) in CO oxidation must be attributed to a disordered Cu-oxide film ultimately formed under the reaction conditions.

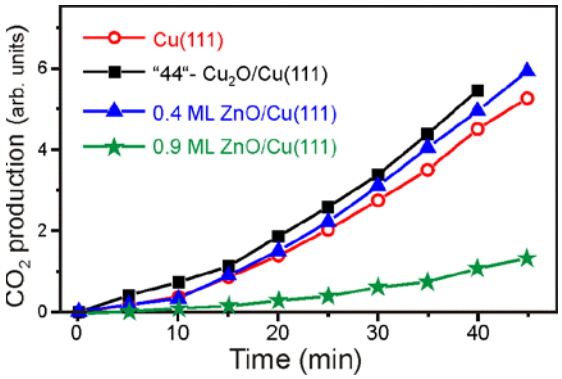

Figure 4. Integrated CO_2 production over Cu(111), well-ordered "44"-Cu_2O/Cu(111), and ZnO(0001)/Cu(111) surfaces as indicated (see text). Reaction conditions: 10 mbar CO, 50 mbar O_2 (He balance to 1 bar); 450 K.

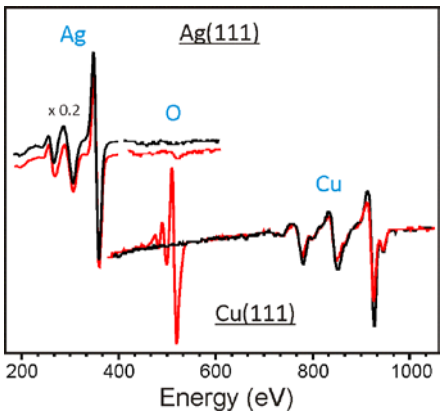

Figure 5. Auger spectra of Ag(111) and Cu(111) surfaces before (black lines) and after (red lines) the CO oxidation reaction. Formation of a CuO_x overlayer is clearly observed on Cu(111), whereas the Ag(111) surface remains metallic.

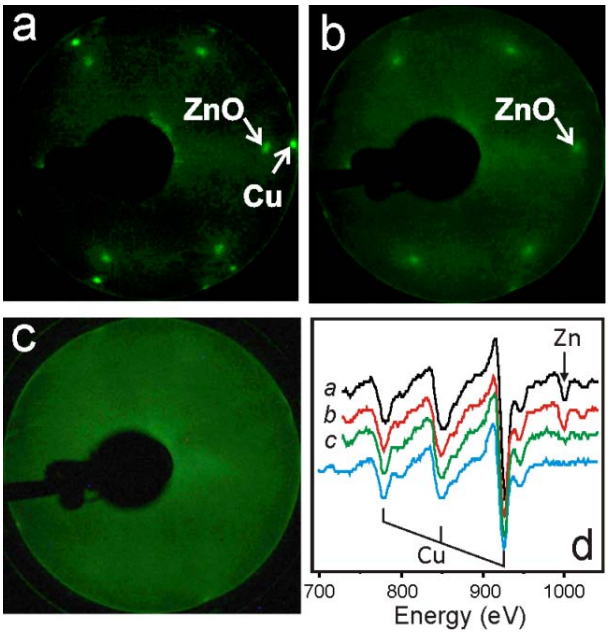

Figure 6. LEED (a-c) and corresponding AES (d) results for the 0.8 ML ZnO/Cu(111) film: as prepared (a), after exposure to the reaction mixture at 300 K for 10 min (b), and 450 K for 1 min (c). The bottom (blue) spectrum in (d) was obtained for the spent catalyst after 30 min of the reaction at 450 K. Cu and Zn Auger transitions are indicated.

As in the case of ZnO/Ag(111), the reactivity tests over ZnO/Cu(111) did not reveal any promotional effect of ZnO on CO oxidation. In fact, the addition of ZnO in large amounts even suppresses reactivity. However, in contrast to the Ag(111)-supported films, post-characterization of the spent ZnO/Cu(111) catalysts by AES showed almost no Zn within 3 nm of

the surface (a typical escape length of electrons at energies of ~ 1000 eV). Since the decomposition temperature of ZnO films (~ 900 K [13, 20]) is much higher than the reaction temperature (450 K), one can safely conclude that ZnO migrates into the Cu crystal bulk rather than sublimes from the surface.

To shed more light on this effect, we have performed LEED and AES measurements on the ZnO film after sequential treatments as shown in Fig. 6. The "as prepared" film shows clear fingerprints of ZnO(0001) in LEED and AES. After the sample has been exposed to the reaction mixture (10 mbar CO, 50 mbar O_2, He balance) at 300 K for 10 min, the Cu(111) spots totally disappear in LEED, while the ZnO(0001) spots remain but become more diffuse. This finding suggests that a disordered CuO_x overlayer is formed under high oxygen pressure even at room temperature. Apparently the Cu-oxide is formed not only on the uncovered Cu(111) surface, but also underneath the ZnO layer; otherwise, the Cu(111) diffraction spots would still be visible in LEED. After the sample was heated to 450 K for ca. 1 min in the reaction mixture, the Auger spectrum showed only a tiny amount of Zn at the surface, and concomitantly the ZnO(0001) pattern disappeared. The ZnO fingerprints totally vanish for longer exposures. Upon exposure to the reaction mixture and subsequent heating to the reaction temperature, it appears that the Cu support is oxidized, and Zn migrates into the crystal bulk through the Cu-oxide layer. As a result, the reactivity is governed by the resultant Cu-oxide film, the formation of which may be affected by ZnO. To explain the rate self-acceleration (Fig. 4), the Cu-oxide film seems to undergo further reaction-induced transformations.

3.3. Reactivity of metal-supported ZnO(0001) films: Comparison

Now we are in position to compare the catalytic behavior of ZnO ultrathin films on Ag(111), Cu(111) and Pt(111). As shown above, the ZnO film on Cu(111) is thermodynamically unstable under reaction conditions at technologically relevant pressures such that the reactivity is governed, in essence, by the ill-defined Cu-oxide film. In contrast, the planar morphology of ZnO films grown on Ag(111) and Pt(111) is maintained in the reaction. For dense ZnO(0001) films, the CO oxidation rate is independent of the metal support, and this rate has turned out to

be the smallest amongst the thin oxide films studied under the same conditions [11]. At sub-monolayer coverages, the ZnO/Pt(111) and ZnO/Ag(111) model catalysts can be represented by a ZnO(0001) bilayer island on a metal support. Previously, a considerable rate enhancement has been observed on Pt(111)-supported films. The structure-reactivity relationships directly showed that the oxide/metal boundary provides the active sites. Such an enhancement is not observed here for the Ag(111)-supported ZnO films.

In attempts to identify the active sites at the oxide/Pt(111) boundaries in CO oxidation, Sun et al. have recently performed a density functional theory (DFT) study of 3d transition-metal oxide monolayer nano-ribbons on Pt(111) [34]. The calculations suggest that coordinatively unsaturated metal cations exposed at the edge of the oxide layer are active for O_2 adsorption and dissociation, and dissociated O readily reacts with CO adsorbed on Pt in close proximity. It should be noted, however, that monolayer MO(111) (M = Mn, Fe, Ni, Co, Zn, etc) films used in these calculations were represented by a close-packed layer of metal cations (bonded to Pt) and a topmost layer of oxygen anions. However, our studies of FeO(111)[10] and ZnO(0001)[13] films on Pt(111) showed that such a monolayer structure is unstable under realistic pressure conditions. Moreover, other DFT studies of ZnO(0001) films on noble metals (Pd(111)[35], Cu(111) [36], and Au(111)[37]) and experimental data available for ZnO/Ag(111)[21] revealed substantial interlayer relaxations such that ultrathin ZnO films resemble the co-planar sheets in the boron nitride (or graphite) structure, and they are only weakly bound to a metal support, in contrast to the models used by Sun et al. [34].

The generally accepted Langmuir-Hinshelwood mechanism for CO oxidation on Pt(111) suggests that CO oxidation at low temperatures is inhibited by strong CO adsorption that blocks O_2 dissociation. Therefore, the rate enhancement observed for ZnO/Pt(111) suggests that ZnO island edges provide reactive O species. According to the above-mentioned calculations by Sun et al. [34] (although this still needs to be proven for a ZnO bilayer), this oxygen binds both to a metal cation of the oxide layer (Zn) and the support (Pt). Since CO adsorbs very weakly on transition metal oxides, it appears that CO, which further reacts with O, adsorbs on Pt(111) near the O species. Assuming that ZnO islands on both Ag(111) and Pt(111) supports are structurally identical (which seems reasonable due to a weak interaction of a ZnO sheet with a

noble metal), the origin of the observed support effect seems to be the adsorption of CO on different metals and of O_2 at the oxide/metal interface. Since CO and O_2 adsorption takes place on different sites which are not competitive, one can apply the model of overlapping states, which asserts that desorption profiles of two reacting entities must overlap for the reaction to occur [38].

It is well documented that both CO and O_2 react very weakly with the Ag(111) surface but strongly with Pt(111). Indeed, CO desorption temperatures (depending on coverage) are roughly 50 K and 450 K for Ag(111)[31] and Pt(111)[39] surfaces, respectively. Certainly, strong CO adsorption (which remains unchanged in the presence of ZnO as shown by DFT [34]) on Pt in the vicinity of the active O species on the ZnO island rim increases its residence time and hence the probability to react. In the case of Ag(111), this probability is strongly diminished as CO adsorbs very weakly.

Regarding the precise nature of active O species, neither experimental data nor DFT calculations for adequate (bilayer) structures are available. Within the model suggested by Sun et al. [34], this oxygen links a Zn^{2+} cation and Pt surface atoms. This oxygen is more weakly bound (by ~ 0.2 eV) than on clean Pt(111). Adopting the same scenario for ZnO/Ag(111), one would expect the O species to be more weakly bound than O on pristine Ag(111). Accordingly, oxygen in the Zn-O-Ag linkages will be more weakly bound than in Zn-O-Pt, since O atoms adsorbs more strongly on Pt(111) than on Ag(111). However, the difference between adsorption energies of atomic O atoms on Ag(111) and Pt(111) as characterized by their desorption temperatures (580 K [30] and 700 K [40], respectively) are relatively small compared to the differences in CO adsorption (50 and 450 K, respectively [31, 39]). Therefore, the above considerations within the model of overlapping states favor the facile reaction on the ZnO/Pt(111) boundary and not on ZnO/Ag(111), in agreement with our experimental results.

3.4. Probing other reactions on ZnO(0001)/Ag(111)

Since ZnO is an important component of commercial methanol synthesis catalysts and is also considered as part of efficient catalysts for the water-gas shift (WGS) and reverse WGS

reactions, we have also examined the catalytic properties of ZnO films on Ag(111) in those reactions. First, we note that in order to exclude water condensation on the room-temperature walls of the reactor and connected gas lines, the partial pressure of water in the system was limited to a few millibars. Second, to be certain that the measured reactivity is attributed to a prepared surface we also inspected different ZnO-free surfaces for comparison.

Figure 7 shows integrated CO_2 production measured for the WGS reaction ($CO + H_2O \rightarrow CO_2 + H_2$) in the mixture of 3 mbar CO, 3 mbar H_2O (He balance to 1 bar) at 500 K. The results show that the clean Ag(111) crystal exhibits the highest activity. Deposition of metallic Cu and Zn (not shown here) and growth of well-ordered ZnO and CuO_x films on Ag(111) prior to the reaction suppress the activity. All catalysts showed deactivation after ca. 10 minutes of reaction. Post-characterization of the spent catalysts by LEED and AES showed that the Ag(111) surface remains essentially unreconstructed, whereas the ZnO films become disordered.

The reverse WGS reaction ($CO_2 + H_2 \rightarrow CO + H_2O$) over both clean Ag(111) and ZnO-covered Ag(111) crystals in the mixture of 50 mbar CO_2 and 50 mbar H_2 (He balance to 1 bar) at 500 K did not show any CO formation, hence indicating no (or negligible) reactivity.

Although the experimental database presented here is rather limited, we can conclude that ZnO films do not show any promotional effect in the WGS and reverse WGS reactions

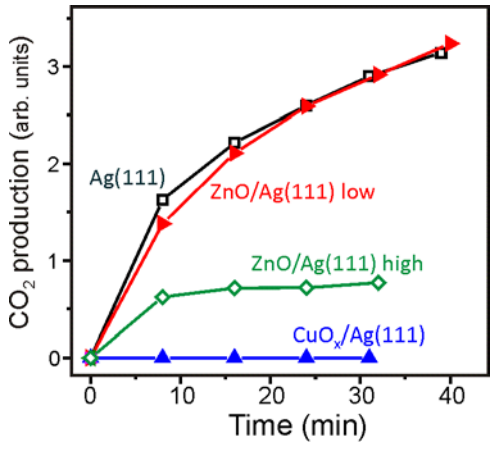

Figure 7. Integrated CO_2 production measured over different surfaces prepared on Ag(111) as indicated. Indexes "low" and "high" mean low and high coverages of ZnO(0001) as judged by AES and LEED. A well-ordered Cu-oxide film (of yet unidentified structure) on Ag(111) was formed by oxidation of a Cu ultrathin film in 10^{-4} mbar O_2 at 750 K. Reaction conditions: 3 mbar CO, 3 mbar H_2O, He balance to 1 bar; 500 K.

under the conditions studied. On the other hand, the promotional effects of ZnO in the WGS reactions are well documented in the literature for real catalysts, although mostly for Cu/ZnO (see, for instance, [16, 17] and references therein). Therefore, our results indicate that ZnO films covering metal particles are not responsible for the high activity commonly observed on real catalysts in those reactions. Assuming that these reactions involve the metal/oxide boundary, the absence of promotional effect on ZnO/metal model catalysts studied here indicates that the "inverse" catalysts do not expose the same sites as "normal", metal/ZnO catalysts. Note also, that the ZnO films become disordered under both WGS and r-WGS reaction conditions, that renders finding the structure-reactivity relationships very difficult even on planar model systems.

4. Conclusions

Ultrathin films of ZnO(0001) were successfully grown on Ag(111) and Cu(111) single crystal surfaces as shown by LEED, AES, and STM. The films, prepared to various coverages, were studied in the CO oxidation reaction at near atmospheric pressures, and their activities were compared to those of the respective pristine metal supports as well as to ZnO/Pt(111) previously studied in our group. On ZnO/Ag(111) and ZnO/Pt(111), the planar ZnO structure is maintained even at high pressures of oxygen. For ZnO/Cu(111), it is shown that ZnO migrates into the crystal bulk under reaction conditions, and the reactivity is governed by the resulting CuO_x overlayer.

In contrast to ZnO/Pt(111), where the enhanced reactivity is observed due to the reaction at the oxide/support boundary, ZnO films on Ag(111) do not show any substantial effect. This is explained by much weaker CO adsorption on Ag(111) as compared to Pt(111), resulting in fewer reactions with O species present at the ZnO/metal boundary.

In addition, the WGS and reverse WGS reactions were examined for ZnO/Ag(111). No promotional effect of ZnO on reactivity was observed under the conditions studied. To some extent, this finding is at variance to catalytic performances of ZnO based catalysts in methanol and WGS reactions showing the exclusive role of ZnO in those reactions. Our "negative" results

may indicate that either (i) ZnO wetting phenomena are not relevant to those reactions, or (ii) the "inverse" (i.e. ZnO/metal) catalysts studied here do not expose those sites present on "normal", metal/ZnO catalysts. In addition, the results revealed that, for the reactions involving water and hydrogen, the ZnO(0001) ultrathin films become unstable under realistic conditions and hence cannot be considered as adequate structural models for such reactions.

Finally, our preliminary studies of ZnO/Pt(111) surfaces by infrared spectroscopy revealed hydroxyl species on the "as prepared" films. Further investigations remain to be done in order to elucidate their role in the reactivity of the ZnO/metal surfaces at elevated pressures.

Acknowledgements

The work has been supported by Fonds der Chemischen Industrie, Deutsche Forschungsgemeinschaft, and Cluster of Excellence "UniCat", in particular through the Northwestern University – CoE "UniCat" collaboration. BHL acknowledges the International Max Planck Research School "Complex surfaces in materials science". MEM was a Fulbright Grantee in the Graduate Fellow Student Program 2011–2012. MEM and MJB were supported in part by US Department of Energy Grant No. DE-FG02-03ER15457. IMNG thanks the Alexander von Humboldt Foundation for a fellowship.

References

1. Freund, H.-J. and G. Pacchioni, *Oxide ultra-thin films on metals: new materials for the design of supported metal catalysts.* Chemical Society Reviews, 2008. **37**(10): p. 2224-2242.
2. Shaikhutdinov, S. and H.-J. Freund, *Ultrathin Oxide Films on Metal Supports: Structure-Reactivity Relations.* Annual Review of Physical Chemistry, 2012. **63**(1): p. 619-633.
3. Giordano, L. and G. Pacchioni, *Oxide Films at the Nanoscale: New Structures, New Functions, and New Materials.* Accounts of Chemical Research, 2011. **44**(11): p. 1244-1252.
4. Netzer, F.P., F. Allegretti, and S. Surnev, *Low-dimensional oxide nanostructures on metals: Hybrid systems with novel properties.* Journal of Vacuum Science & Technology B: Microelectronics and Nanometer Structures, 2010. **28**(1): p. 1-16.
5. Lundgren, E., et al., *Surface oxides on close-packed surfaces of late transition metals.* Journal of Physics: Condensed Matter, 2006. **18**(30): p. R481.

6. Over, H., et al., *Atomic-Scale Structure and Catalytic Reactivity of the RuO2(110) Surface.* Science, 2000. **287**(5457): p. 1474-1476.
7. Martynova, Y., et al., *Low Temperature CO Oxidation on Ruthenium Oxide Thin Films at Near-Atmospheric Pressures.* Catalysis Letters, 2012. **142**(6): p. 657-663.
8. Over, H., *Surface Chemistry of Ruthenium Dioxide in Heterogeneous Catalysis and Electrocatalysis: From Fundamental to Applied Research.* Chemical Reviews, 2012.
9. Martynova, Y., et al., *CO oxidation over monolayer manganese oxide films on Pt(111).* Catalysis Letters, 2013. **in press**.
10. Sun, Y.N., et al., *Monolayer iron oxide film on platinum promotes low temperature CO oxidation.* Journal of Catalysis, 2009. **266**(2): p. 359-368.
11. Martynova, Y., S. Shaikhutdinov, and H.-J. Freund, *CO Oxidation on Metal-Supported Ultrathin Oxide Films: What Makes Them Active?* Chemcatchem, 2013. **5**(8): p. 2162-2166.
12. Lewandowski, M., et al., *Promotional effect of metal encapsulation on reactivity of iron oxide supported Pt catalysts.* Applied Catalysis a-General, 2011. **391**(1-2): p. 407-410.
13. Martynova, Y., et al., *CO oxidation over ZnO films on Pt(111) at near-atmospheric pressures.* Journal of Catalysis, 2013. **301**(0): p. 227-232.
14. Hayek, K., et al., *Surface reactions on inverse model catalysts: CO adsorption and CO hydrogenation on vanadia- and ceria-modified surfaces of rhodium and palladium.* Topics in Catalysis, 2000. **14**(1-4): p. 25-33.
15. Schoiswohl, J., et al., *Vanadium oxide nanostructures on Rh(1 1 1): Promotion effect of CO adsorption and oxidation.* Surface Science, 2005. **580**(1–3): p. 122-136.
16. Behrens, M., et al., *The Active Site of Methanol Synthesis over Cu/ZnO/Al2O3 Industrial Catalysts.* Science, 2012. **336**(6083): p. 893-897.
17. Grunwaldt, J.D., et al., *In Situ Investigations of Structural Changes in Cu/ZnO Catalysts.* Journal of Catalysis, 2000. **194**(2): p. 452-460.
18. Kanai, Y., et al., *Evidence for the migration of ZnOx in a Cu/ZnO methanol synthesis catalyst.* Catalysis Letters, 1994. **27**(1-2): p. 67-78.
19. Naumann d'Alnoncourt, R., et al., *The influence of strongly reducing conditions on strong metal-support interactions in Cu/ZnO catalysts used for methanol synthesis.* Physical Chemistry Chemical Physics, 2006. **8**(13): p. 1525-1538.
20. Kourouklis, H.N. and R.M. Nix, *The growth and structure of ZnOx overlayers on low index silver surfaces.* Surface Science, 1994. **318**(1–2): p. 104-114.
21. Tusche, C., H.L. Meyerheim, and J. Kirschner, *Observation of Depolarized ZnO(0001) Monolayers: Formation of Unreconstructed Planar Sheets.* Physical Review Letters, 2007. **99**(2): p. 026102.
22. Claeyssens, F., et al., *Growth of ZnO thin films-experiment and theory.* Journal of Materials Chemistry, 2005. **15**(1): p. 139-148.
23. Sano, M., et al., *Oxidation of a Zn-deposited Cu(1 1 1) surface studied by XPS and STM.* Surface Science, 2002. **514**(1–3): p. 261-266.
24. Thomsen, E.V., M. Christiansen, and J. Onsgaard, *The growth of Zn and ZnOx on Cu(111).* Applied Surface Science, 1992. **62**(3): p. 189-194.
25. Onsgaard, J. and J.A. Bjo/rn, *Growth and reactivity of ZnOx on Cu(111).* Journal of Vacuum Science & Technology A, 1993. **11**(4): p. 2179-2185.
26. Fu, S.S. and G.A. Somorjai, *A comparative study of zinc oxide overlayers on copper (311), Cu(110), and a high defect concentration Cu(111).* Langmuir, 1992. **8**(2): p. 518-524.
27. Campbell, C.T., K.A. Daube, and J.M. White, *Cu/ZnO(0001̄) and ZnOx/Cu(111): Model catalysts for methanol synthesis.* Surface Science, 1987. **182**(3): p. 458-476.
28. McBriarty, M.E., et al., *Surface structure of ZnO films on Ag(111).* in preparation.

29. Steurer, W., et al., *Scanning tunneling microscopy imaging of NiO(100)(1 × 1) islands embedded in Ag(100).* Surface Science, 2012. **606**(9–10): p. 803-807.
30. Campbell, C.T., *Atomic and molecular oxygen adsorption on Ag(111).* Surface Science, 1985. **157**(1): p. 43-60.
31. Hansen, W., M. Bertolo, and K. Jacobi, *Physisorption of CO on Ag(111): investigation of the monolayer and the multilayer through HREELS, ARUPS, and TDS.* Surface Science, 1991. **253**(1–3): p. 1-12.
32. Liu, B.H., S. Shaikhutdinov, and H.J. Freund, *Growth of crystalline ZnO films on Cu(111).* in preparation.
33. Jensen, F., et al., *Oxidation of Cu(111): two new oxygen induced reconstructions.* Surface Science Letters, 1991. **259**(3): p. L774-L780.
34. Sun, D., et al., *Theoretical Study of the Role of a Metal–Cation Ensemble at the Oxide–Metal Boundary on CO Oxidation.* The Journal of Physical Chemistry C, 2012. **116**(13): p. 7491-7498.
35. Weirum, G., et al., *Growth and Surface Structure of Zinc Oxide Layers on a Pd(111) Surface.* The Journal of Physical Chemistry C, 2010. **114**(36): p. 15432-15439.
36. Schott, V., et al., *Chemical Activity of Thin Oxide Layers: Strong Interactions with the Support Yield a New Thin-Film Phase of ZnO.* Angewandte Chemie International Edition, 2013. **52**(45): p. 11925-11929.
37. Deng, X., et al., *Growth of Single- and Bilayer ZnO on Au(111) and Interaction with Copper.* The Journal of Physical Chemistry C, 2013. **117**(21): p. 11211-11218.
38. Doyle, A.M., S.K. Shaikhutdinov, and H.J. Freund, *Alkene chemistry on the palladium surface: nanoparticles vs single crystals.* Journal of Catalysis, 2004. **223**(2): p. 444-453.
39. Steininger, H., S. Lehwald, and H. Ibach, *On the adsorption of CO on Pt(111).* Surface Science, 1982. **123**(2–3): p. 264-282.
40. Steininger, H., S. Lehwald, and H. Ibach, *Adsorption of oxygen on Pt(111).* Surface Science, 1982. **123**(1): p. 1-17.

Supplementary Information

to the paper “Reactivity of ultra-thin ZnO films supported by Ag(111) and Cu(111): A comparison to ZnO/Pt(111)”” authored by Q. Pan, et al.

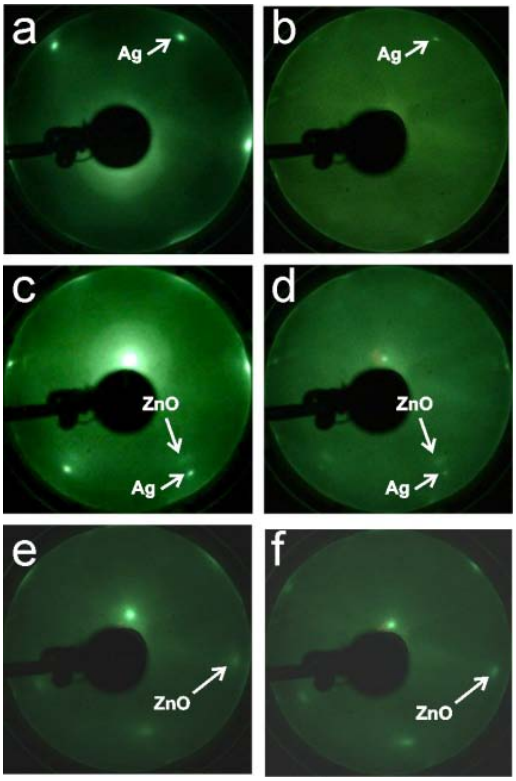

Figure S1. LEED patterns of clean Ag(111) (a,b) and ZnO/Ag(111) films at low (c,d) and high (e,f) coverage before (left panel) and after (right panel) CO oxidation reaction.

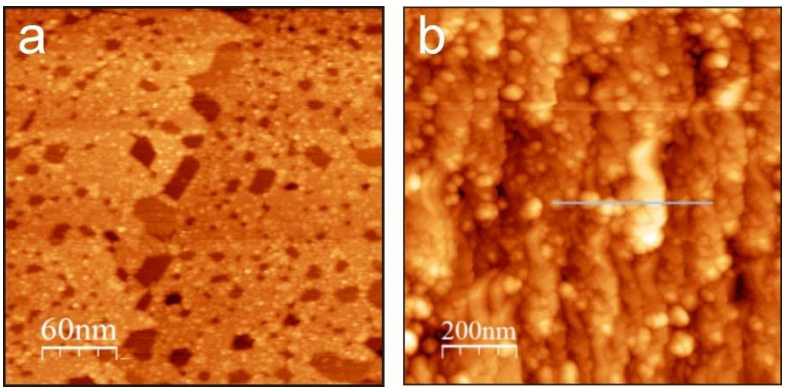

Figure S2. STM images of ZnO(0001) films on Ag(111) (a) and Cu(111) (b) after CO oxidation reaction. Substantial surface restructuring occurs for ZnO grown on Cu(111) (b), whereas the film maintains the planar structure when deposited on Ag(111).